

Particle Diameter Influences Adhesion under Flow

Vivek R. Shinde Patil,^{*†} Craig J. Campbell,[†] Yang H. Yun,[†] Steven M. Slack,[†] and Douglas J. Goetz^{*†}

^{*}The Department of Chemical Engineering, Ohio University, Athens, Ohio 45701 and [†]The Department of Biomedical Engineering, The University of Memphis, Memphis, Tennessee 38152, USA

ABSTRACT The diameter of circulating cells that may adhere to the vascular endothelium spans an order of magnitude from $\sim 2 \mu\text{m}$ (e.g., platelets) to $\sim 20 \mu\text{m}$ (e.g., a metastatic cell). Although mathematical models indicate that the adhesion exhibited by a cell will be a function of cell diameter, there have been few experimental investigations into the role of cell diameter in adhesion. Thus, in this study, we coated 5-, 10-, 15-, and 20- μm -diameter microspheres with the recombinant P-selectin glycoprotein ligand—1 construct 19.ek.Fc. We compared the adhesion of the 19.ek.Fc microspheres to P-selectin under in vitro flow conditions. We found that 1) at relatively high shear, the rate of attachment of the 19.ek.Fc microspheres decreased with increasing microsphere diameter whereas, at a lower shear, the rate of attachment was not affected by the microsphere diameter; 2) the shear stress required to set in motion a firmly adherent 19.ek.Fc microsphere decreased with increasing microsphere diameter; and 3) the rolling velocity of the 19.ek.Fc microspheres increased with increasing microsphere diameter. These results suggest that attachment, rolling, and firm adhesion are functions of particle diameter and provide experimental proof for theoretical models that indicate a role for cell diameter in adhesion.

INTRODUCTION

Cellular adhesion to vascular endothelium in the fluid-dynamic environment of the circulation is an important aspect of many physiological and pathological processes. Examples include platelet adhesion during the later stages of atherosclerosis (Ross, 1999), leukocyte adhesion during recruitment to a site of tissue injury (Springer, 1994), and cancer cell adhesion during metastasis (Giavazzi, 1996). The diameters of these various adhering cells span an order of magnitude from $2 \mu\text{m}$ (the approximate size of a platelet) to $20 \mu\text{m}$ (the size of some metastasizing cells) with leukocytes (7–10 μm) falling within this range. It is important to recognize that the adhesion exhibited by a cell may be a function of the diameter of the cell. Examples of where a clear understanding of the role of cell diameter in adhesion is necessary include 1) comparing platelet adhesion (Frenette et al., 1995) to leukocyte adhesion (Lawrence and Springer, 1991), 2) experimental adhesion assays with ligand transfectants (e.g., using an $\sim 10\text{-}\mu\text{m}$ -diameter mammalian cell line transfected with a platelet ligand (Fredrickson et al., 1998)), and 3) elucidating the relative importance of mechanical trapping versus specific adhesion in cancer-cell arrest in a secondary organ (Scherbarth and Orr, 1997; Chambers et al., 1995; Goetz et al., 1996a,b; McCarty et al., 2000).

In considering the role of cell diameter in adhesion, it is helpful to realize that adhesion under flow is a rather broad term, encompassing several adhesive states (Hammer and Apte, 1992; Goetz et al., 1996a). The initial attachment of the cell from the free stream to the endothelium is often referred to as attachment (Goetz et al., 1996a), capture

(Munn et al., 1995), or initial tethering (Lawrence et al., 1994). Subsequent to attachment, the cell may remain stationary on the endothelium (exhibit firm adhesion), may release back into the free stream (detachment), or may continue to move in the direction of flow at a low velocity (roll). Thus, cell adhesion can be categorized into several types of adhesive behavior, including attachment, rolling, and firm adhesion.

Mathematical models of firm adhesion strongly suggest that the diameter of an adhering cell will significantly influence the adhesion of the cell to the endothelium. In the ideal case of a nondeformable spherical cell firmly adherent to an adhesive substrate under Couette flow, the force and torque exerted on the cell by the flow of the fluid will be proportional to the square and the cube of the cell diameter, respectively (Goldman et al., 1967). For the cell to remain firmly adherent, this disruptive force and torque must be balanced by an adhesive force mediated by receptor–ligand bonds occurring in the area of contact between the adherent cell and the adhesive substrate. It is reasonable to argue that the adhesive force will be a function of the size of the contact area. Because the size of the contact area is a function of the diameter of the cell (Cozens-Roberts et al., 1990), it appears that both the disruptive and adhesive forces acting on the adherent cell will be a function of the diameter of the cell.

Using these ideas and the model by Hammer and Lauffenburger (1987), Cozens-Roberts et al. (1990) derived an expression for the shear stress required to remove an adherent particle from an adhesive substrate. They termed this parameter the critical shear stress, Sc , and deduced that Sc can be estimated by the relationship $K(\sin \Theta)^3$. Here, K incorporates the thermodynamic properties of the receptor–ligand pair, the temperature, and the surface densities of the receptor and ligand. Θ is the angle of the contact area over which a receptor–ligand bond can form. Because Θ is a

Received for publication 15 May 2000 and in final form 19 January 2001.

Address reprint requests to Douglas J. Goetz, Ohio University, The Department of Chemical Engineering, 172 Stocker Center, Athens, OH 45701. Tel.: 740-593-1494; Fax: 740-593-0873; E-mail: goetzd@ohio.edu.

© 2001 by the Biophysical Society

0006-3495/01/04/1733/11 \$2.00

function of the diameter of the particle (Cozens-Roberts et al., 1990), the analysis of Cozens-Roberts suggests that Sc will be a function of the diameter of the cell.

Clearly then, it is reasonable to suspect that cell diameter affects firm adhesion. A review of mathematical models of cell attachment and rolling also suggests that cell diameter will affect attachment and rolling (Hammer and Lauffenburger, 1987; Hammer and Apte, 1992; Chang and Hammer, 1999). In addition to the direct effect that cell diameter may have on adhesion (i.e., the direct effect on the adhesive mechanics just described), cell diameter will also affect the transport of the cell by influencing the diffusion of the cell (Goldsmith and Turitto, 1986) and the hydrodynamic effect of the vessel wall on the cell velocity (Goldman et al., 1967).

Although theory clearly predicts that cell diameter will affect adhesion and that the size range of cells that may bind to the endothelium is quite broad, there have been few experimental studies aimed at investigating the relationship between cell diameter and adhesion. Wattenbarger et al. (1990) studied the adhesion of glycoprotein liposomes to lectin-coated surfaces in shear flow. Although this study was not intended to be a thorough investigation into the relationship between cell diameter and adhesion, the results did suggest that particle diameter affects adhesion. In particular, Wattenbarger et al. found that the larger-diameter glycoprotein liposomes had a greater propensity to detach from the lectin-coated substrate compared to the smaller-diameter glycoprotein liposomes. It should be noted that they did not know if the surface density of glycoprotein on the liposomes was similar for each diameter liposome, and they did not probe all adhesive states (e.g., attachment and rolling).

In summary, it is reasonable to postulate, and indeed mathematical models predict, that the observed adhesion between a cell and an adhesive substrate will be a function of the diameter of the cell. The experimental data investigating this issue is limited. Thus, in this study, we used *in vitro* flow assays to probe the role of cell diameter in adhesion. Because cells have attributes, in addition to diameter, that vary from one cell type to another and may significantly affect the adhesion of the cell, we investigated the role of cell diameter using ligand-coated microspheres. Specifically, we used 5-, 10-, 15-, and 20- μm -diameter microspheres (Goetz et al., 1997) coated with equivalent surface densities of a recombinant P-selectin glycoprotein ligand-1 (PSGL-1) construct termed 19.ek.Fc. We then compared the adhesion of the different sized 19.ek.Fc microspheres to P-selectin under *in vitro* flow conditions that mimic, in part, flow conditions present *in vivo*.

MATERIALS AND METHODS

Materials and preparation of 19.ek.Fc microspheres

HBSS with Ca^{2+} and Mg^{2+} (HBSS+), was from Biowhittaker (Walkersville, MD). Human IgG₁ and bovine serum albumin (BSA) were from

Sigma (St. Louis, MO). Protein A was from Zymed (San Francisco, CA). Leukocyte function-blocking murine anti-P-selectin mAb, HPDG2/3 (IgG₁) (Sako et al., 1993), nonblocking murine anti-P-selectin mAb, HPDG2/1 (IgG₁) (Sako et al., 1993), murine blocking anti-PSGL-1 (Pharmingen, San Diego, CA) were used as purified IgG₁. Recombinant P-selectin consisting of the full extracellular region of P-selectin has been previously described (Sako et al., 1993, 1995). The PSGL-1 molecule used in this study is a chimera consisting of a truncated extracellular region of mature PSGL-1 (the first 19 amino acids of mature PSGL-1) linked to an enterokinase cleavage site, which, in turn, is linked to the heavy chain CH2-CH3 (Fc) region of human IgG₁. This construct is referred to as 19.ek.Fc and has been previously described (Goetz et al., 1997; Sako et al., 1995). The 19.ek.Fc construct was coupled to 5-, 10-, 15-, and 20- μm -diameter polystyrene microspheres (Bangs Laboratories Inc., Fishers, IN) by protein A, as previously described (Goetz et al., 1997). The standard deviation of the diameter of the microspheres was 0.07, 0.1, 0.42, and 0.33 μm , respectively. The coating concentration of the 19.ek.Fc solution was 20 $\mu\text{g}/\text{ml}$. Note that when coupling the 19.ek.Fc to the microspheres, the amount of 19.ek.Fc added per protein A microsphere surface area was the same for each sized microsphere. Thus, per 5 μl of the 19.ek.Fc coating solution, 4×10^6 5- μm microspheres, 1×10^6 10- μm microspheres, 4.44×10^5 15- μm microspheres, and 2.5×10^5 20- μm microspheres were coated. Coating in this manner resulted in microspheres that had similar surface densities of 19.ek.Fc (see Fig. 2 B). BSA coated microspheres were prepared by incubating the microspheres in HBSS+, 1% BSA at least 1 hr before use in an adhesion assay. The mAbs to P-selectin, 19.ek.Fc construct, and soluble P-selectin were a generous gift from Dr. Raymond T. Camphausen (Genetics Institute; Cambridge, MA).

Parallel plate flow chamber

The parallel plate flow chamber (Glycotech, Rockville, MD) is similar to that used by McIntire, Smith, and colleagues (Gopalan et al., 1996) and consists of a Plexiglas flow deck that fits inside a 35-mm tissue culture dish. Our particular flow set-up has been described previously (Crutchfield et al., 2000). In brief, the flow field is defined by a gasket that sits between the flow deck and the 35-mm dish. The shear stress at the bottom surface of the flow chamber is given by $\tau = 3Q\mu/2wh^2$ where Q is the volumetric flow rate, μ is the viscosity, $2h$ is the height (0.2 mm) of the flow field, and w is the width (0.5 cm) of the flow field. The volumetric flow rate was adjusted to obtain the desired shear stress. After assembly, the flow chamber was placed on an inverted microscope connected to a CCD videocamera, VCR, and monitor. The 35-mm dish was rinsed with buffer, and the flow of the microspheres ($1 \times 10^6/\text{ml}$ in HBSS+, 0.5% BSA) initiated. Experiments were carried out at room temperature (24°C).

Preparation of P-selectin substrates for use in the adhesion assay

A silicon ring (Unisyn Technologies, Hopkinton, MA) with an inner diameter of 6 mm was placed on 35-mm tissue-culture dishes (Corning, Corning, NY). The inner region of the ring was outlined on the reverse side of the tissue culture dishes. 35 μl of soluble P-selectin (diluted to 20 $\mu\text{g}/\text{ml}$ in HBSS) or HBSS alone (negative control) was placed inside the rings. The dishes were incubated at 4°C overnight (in a humidified chamber to avoid buffer evaporation), washed, and the entire dish flooded with HBSS+, 1% BSA. The dishes were incubated in HBSS+, 1% BSA at least 30 min prior to the adhesion assay. BSA-coated dishes (negative controls) were prepared by adding 1 ml HBSS+, 1% BSA to the bottom surface of 35-mm tissue-culture dishes at least 30 min prior to the adhesion assay.

mAb blocking

In certain experiments, the P-selectin-coated surface was treated with mAbs to P-selectin (10 $\mu\text{g}/\text{ml}$) 15 min prior to the adhesion assays. For

these experiments, the 19.ek.Fc microspheres were incubated in 200 $\mu\text{g}/\text{ml}$ human IgG₁ before use in the adhesion assay. This prevents microsphere-bound protein A from binding to the Fc region of the mAb bound to P-selectin on the substrate. In certain experiments, the 19.ek.Fc microspheres were pretreated with mAb KPL1 (anti-PSGL-1) 15 min prior to the adhesion assay. In all cases, the number of microspheres present after 2 min of flow was determined in eight different fields of view. These values were averaged and divided by the area of the field of view to give the number of microspheres present/mm². This represented an $n = 1$. The entire experiment was done at least three times and the results averaged to give the presented data.

Measuring microsphere attachment

After assembling the flow chamber, the microscope objective was positioned at the first field of view (the one closest to the inlet) coated with P-selectin. After a short rinse, the flow of 19.ek.Fc microspheres was initiated. The number of 19.ek.Fc microspheres adherent to the surface in the field of view was determined as a function of time. Plots of the number of 19.ek.Fc microspheres bound per unit surface area versus time resulted in curves that were initially linear. As the experiment progressed, the rate of increase in the number of adherent 19.ek.Fc microspheres decreased, apparently due to the surface becoming saturated with microspheres. The initial portion of this curve (i.e., where the rate of attachment appeared to be independent of bound microspheres) was used along with linear regression to determine the effective rate of attachment, k_c . The effective rate of attachment is the rate at which microspheres attach to the P-selectin surface, i.e., go from the free stream velocity to being in an adhesive state (either rolling or firmly adherent) on the P-selectin surface. To correct k_c for the effect of microsphere diameter on delivery to the bottom surface of the flow chamber, the number of microspheres that passed through the field of view "near" the bottom surface of the flow chamber (as indicated by their lower velocity) was determined. For the 75-s⁻¹ data, this number was used along with k_c to calculate a percent adhesion. Because the microspheres were moving too fast at 400 and 600 s⁻¹ to allow an accurate determination of the number of microspheres near the surface, the attachment data could not be corrected for transport at these higher shear rates. Thus, k_c values were used rather than percent adhesion at these shear rates.

Determination of percent firmly adherent

Suspensions containing 19.ek.Fc microspheres were perfused over the P-selectin surfaces at 0.5 dynes/cm². After 10 min of flow, the shear stress was increased in steps. Each level of shear stress was maintained for 1 min for shear stresses ≤ 10 dynes/cm² and for thirty seconds for shear stresses > 10 dynes/cm². 19.ek.Fc microspheres that did not exhibit any motion in the direction of flow within a 5-s time period selected in the middle of the each shear stress interval, were scored as firmly adherent. In certain control experiments, the detachment of 19.ek.Fc microspheres from BSA-coated plastic or the detachment of BSA microspheres from P-selectin-coated surfaces was measured. In this case, the microspheres were drawn into the flow chamber and the flow stopped. After a 10-min incubation, the flow was slowly and smoothly reinitiated. Before reinitiation of the flow, the number of microspheres present on the surface was determined. Immediately after reinitiation of the flow, the number of microspheres firmly adherent was determined.

Determination of the rolling velocity

Recorded data at each shear stress was analyzed for 5 s. 19.ek.Fc microspheres that exhibited a motion in the direction of flow within this time interval were scored as rolling. To evaluate the rolling velocity, the distance traversed by a rolling 19.ek.Fc microsphere in the 5-s interval was

determined. This was divided by 5 s to yield the microsphere rolling velocity. This procedure was extended to all the 19.ek.Fc microspheres within a field of view.

Radiolabeling of protein A and IgG₁

Protein A and human IgG₁, κ were radiolabeled with ¹²⁵I (Amersham, Arlington Heights, IL) by the IODOGEN method using the IODO-BEADS (Pierce Chemical Co., Rockford, IL) iodination reagent. Labeled proteins were separated from unincorporated ¹²⁵I by gel filtration using a Sephadex G-25 column (Pharmacia, Uppsala, Sweden). The concentration of labeled protein was determined using a spectrophotometer (Molecular Devices, Sunnyvale, CA) by measuring the absorption at 280 nm. The extinction coefficients, $E_{280\text{nm}}^{1\%}$, were 2.0 for Protein A and 14 for IgG₁. The radiolabeled solutions were aliquoted and frozen after iodination.

Adsorption of protein A for radiolabeling experiments

Polystyrene microspheres ($\sim 3.0 \times 10^6$ for 10- μm and $\sim 1.2 \times 10^7$ for 5- μm) were washed with 0.1 M NaHCO₃ buffer. Afterwards, the microspheres were divided into three identical aliquots, centrifuged, and the supernatants removed. Each aliquot was resuspended in 40 μL of ¹²⁵I-Protein A (diluted to 0.3 mg/mL, activity of 10,000 cpm/ μg in NaHCO₃), incubated overnight at room temperature, and washed six times with HBSS+ with 1% BSA. The radioactivity of the microsphere samples was determined with a γ counter (Packard, Meriden, CT) and the number of microspheres in each sample counted. These two values were used to determine the amount of protein A adsorbed per cm². The triplicate samples were averaged to give the result for a single experiment. The entire experiment was done three times, and the resulting three values averaged to give the presented data.

IgG₁ standard curve

Microspheres were washed in 0.1 M NaHCO₃, resuspended in protein A (0.3 mg/ml in 0.1 M NaHCO₃), incubated overnight, and washed with HBSS+ 1% BSA. Note that, in this case, the protein A was not radiolabeled. The microspheres were resuspended in HBSS+, 1% BSA, then divided into equal-portion samples ($\sim 2.0 \times 10^6$ per sample for 10- μm and $\sim 8.0 \times 10^6$ per sample for 5- μm). The samples were centrifuged, the supernatant removed, and the microspheres resuspended in 10 μL human IgG₁ solution. The concentration of IgG₁ ranged from 100 to 12.5 $\mu\text{g}/\text{mL}$ in HBSS+, 1% BSA and the activity of the 100 $\mu\text{g}/\text{mL}$ IgG₁ was 10,000 cpm/ μg . Triplicate samples of each IgG₁ concentration were made. The microspheres were incubated for 1 h with agitation and washed six times with HBSS+ 1% BSA. The radioactivity of the microsphere samples was determined, and the number of microspheres in each sample counted. These two values were used to determine the amount of IgG₁ bound per cm². The entire experiment was done twice, and the results from the two experiments averaged to give the data shown.

Statistics

When comparing two means, statistical analyses were done by unpaired Student's *t*-test of the means. In cases of multiple groups, we performed a single-factor ANOVA and, if appropriate, subsequently a Dunnett's test for multiple comparisons against a single control. To check for factor interactions (i.e., shear and microsphere diameter) we used a two-factor randomized-block design ANOVA. Error bars indicate standard deviations unless otherwise noted.

RESULTS

Microspheres coated with a recombinant PSGL-1 construct, 19.ek.Fc, attach, roll, and firmly adhere to P-selectin adsorbed to tissue-culture plastic

The leukocyte adhesion molecule P-selectin glycoprotein ligand-1 (PSGL-1) has been shown to mediate granulocyte attachment and rolling on P-selectin (Patel and McEver, 1997). Previously, we demonstrated that 10- μ m-diameter microspheres coated with the recombinant PSGL-1 construct, 19.ek.Fc, attach and roll on cell lines expressing P-selectin (Goetz et al., 1997). The 19.ek.Fc construct consists of the first 19 amino acids of mature PSGL-1, including the binding site for P-selectin, linked to an enterokinase cleavage site, which, in turn, is linked to the Fc region of human IgG₁ (Sako et al., 1995). We coupled the 19.ek.Fc construct to polystyrene microspheres via protein A as previously described (Goetz et al., 1997). Coupling via protein A allows for the correct orientation of the 19.ek.Fc construct on the microspheres, i.e., the Fc portion bound to the protein A and the PSGL-1 portion of the construct oriented away from the microsphere and available for binding to P-selectin.

In preliminary studies, we found that 19.ek.Fc microspheres attach to soluble purified P-selectin adsorbed to tissue-culture plastic, and, subsequent to attachment, the 19.ek.Fc microspheres either rolled or firmly adhered, depending on the concentration of 19.ek.Fc on the microspheres and the shear stress (data not shown). Thus, we chose to use the 19.ek.Fc microspheres to investigate the

role of particle diameter in adhesion because this system 1) exhibits a range of adhesive states, (including attachment, rolling, and firm adhesion) at physiologically relevant shear stresses, 2) involves a physiologically relevant ligand-receptor pair, 3) contains a minimal level of extraneous factors that could affect adhesion (e.g., cellular surface topology [von Andrian et al., 1995], cellular deformation [Dong et al., 1999]), and 4) contains a minimal number of variables that could vary from experiment to experiment.

As shown in Fig. 1 A, the adhesion of the 19.ek.Fc microspheres to P-selectin adsorbed to tissue culture plastic appears to be specific, because: 1) 19.ek.Fc microspheres attached to adsorbed P-selectin but not to adsorbed BSA (negative control), 2) the attachment to P-selectin was ablated by a function-blocking mAb to P-selectin but not by a nonfunction-blocking mAb to P-selectin, 3) the attachment to P-selectin was ablated by a function-blocking mAb to PSGL-1, and 4) human IgG₁-coated microspheres did not attach to adsorbed P-selectin. In addition, we found that 19.ek.Fc microspheres that were allowed to settle onto BSA-coated plastic under static conditions and BSA microspheres that were allowed to settle onto P-selectin-coated plastic under static conditions were immediately removed from the substrate with the onset of flow (Fig. 1, B and C).

The 19.ek.Fc microspheres have equivalent surface densities of 19.ek.Fc

To rationally interpret the adhesion data in terms of microsphere diameter, it is necessary that the surface concentra-

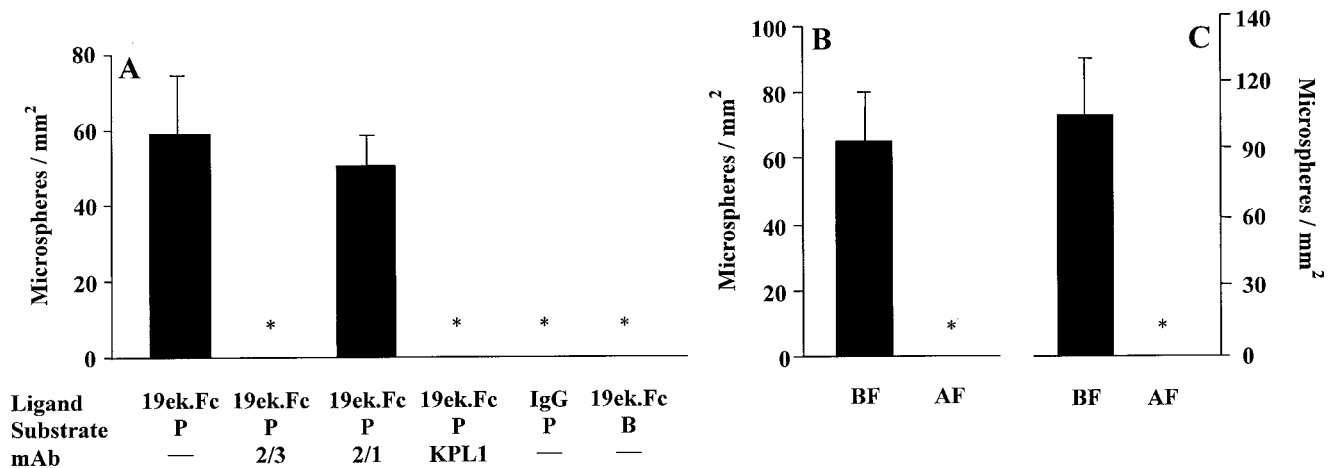


FIGURE 1 19.ek.Fc microspheres exhibit specific adhesion to P-selectin. (A) 10- μ m 19.ek.Fc or human IgG₁ microspheres were perfused over 35-mm dishes coated with P-selectin or BSA (negative control). In certain cases, the substrate or the microspheres were pretreated with mAbs. Legend: Ligand, which molecule was on the microsphere; Substrate, coating the 35-mm dishes with P-selectin (P) or BSA (B); mAb, pretreatment of the microsphere (KPL-1) or substrate (2/3 and 2/1) with the indicated mAb (2/3, HPDG2/3; 2/1, HPDG2/1); $n = 3$; * $p < 0.01$ compared to left-most bar. (B) 19.ek.Fc microspheres were allowed to settle onto BSA-coated 35-mm dishes under no flow conditions for 10 min. After the incubation, the flow was slowly and smoothly reinitiated. Immediately after reinitiation of flow, the number of 19.ek.Fc microspheres remaining bound to the surface was determined. (C) BSA microspheres were allowed to settle onto P-selectin under no flow conditions for 10 min. After the incubation, the flow was slowly and smoothly reinitiated. Immediately after reinitiation of flow, the number of BSA microspheres remaining bound to the surface was determined. Legend for (B) and (C): BF, before flow; AF, after flow. $n = 3$; * $p < 0.01$. All results shown are for 10- μ m microspheres. Similar results were obtained with 5-, 15-, and 20- μ m microspheres.

tion of 19.ek.Fc on the microspheres be equivalent for the different sized microspheres. Assays conducted with radiolabeled protein A revealed that the polystyrene microspheres adsorb ~ 150 ng/cm² of protein A (Fig. 2A). In preparing the different sized 19.ek.Fc microspheres, we

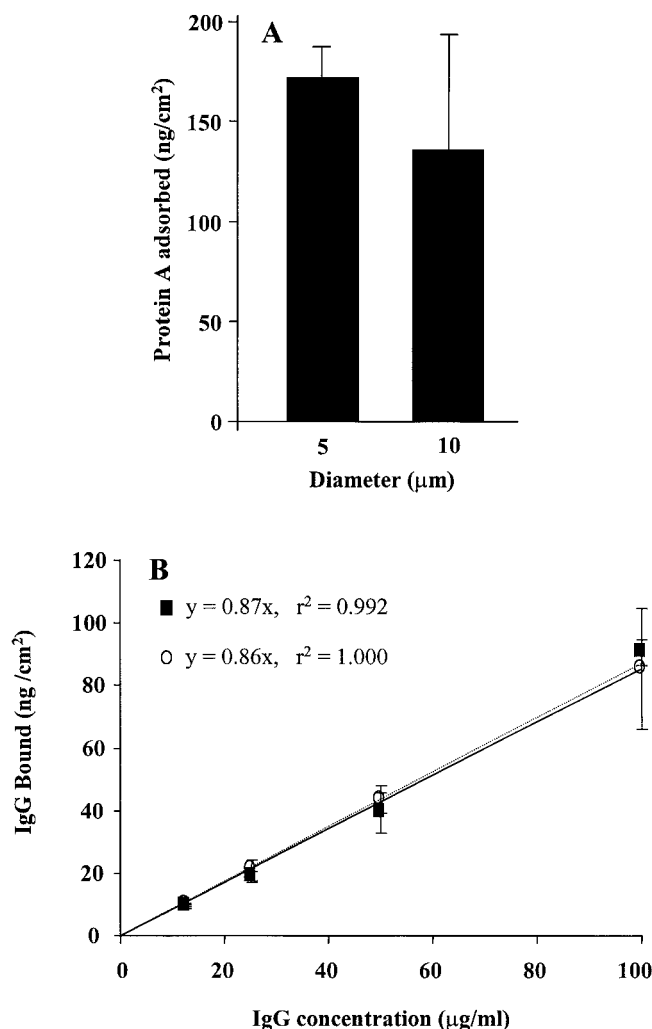


FIGURE 2 Radiolabeling assays to quantify binding of protein A and IgG₁ to polystyrene microspheres. (A) 5- and 10-µm-diameter microspheres were incubated in buffer containing radiolabeled protein A. After extensive washing, the radioactivity in each sample was determined, and, from this value and knowledge of the number of microspheres in each sample, the surface density of protein A on the microspheres was determined. The 5- and 10-µm microspheres adsorb statistically similar levels of protein A per unit area. Preliminary data (not shown) revealed that the amount of protein A used to coat the microspheres resulted in saturation of the microspheres with protein A ($n = 3$). (B) 5- and 10-µm microspheres precoated with saturating levels of protein A were incubated in increasing concentrations of radiolabeled human IgG₁. After extensive washing, the radioactivity of each sample was determined, and, from this value and knowledge of the number of microspheres in each sample, the surface density of human IgG₁ was determined. The assays revealed that the surface density of human IgG₁ on the 5-µm microspheres was statistically similar to that on the 10-µm microspheres. (Legend: black boxes, 10-µm microspheres; white circles, 5-µm microspheres; $n = 2$).

coupled the 19.ek.Fc to the protein A microspheres in such a way that the amount of 19.ek.Fc added per protein A microsphere surface area was the same for each sized microsphere. Under these conditions, it is reasonable to assume that the resulting 19.ek.Fc surface density on the microspheres would be the same for each sized microsphere. To check this assumption, we conducted radiolabeling assays with two sets of microspheres, the 5- and 10-µm-diameter microspheres. Because the 19.ek.Fc was available to us in limited quantities, we used human IgG₁ in this assay rather than 19.ek.Fc. Radiolabeling assays revealed that the surface density of human IgG₁ was statistically similar on the 5- and 10-µm-diameter IgG₁ microspheres (Fig. 2B). We used the same protocols to generate each of the 19.ek.Fc microspheres, making sure that the amount of 19.ek.Fc added per microsphere surface area was identical for each sized microsphere and using 20 µg/ml of 19.ek.Fc. Under these conditions, based on the data in Fig. 2, it is reasonable to conclude that the surface density of 19.ek.Fc on the 5-, 10-, 15-, and 20-µm-diameter microspheres are similar.

Microsphere diameter affects the rate of attachment under flow

We would ultimately like to understand the role of particle diameter in adhesion *in vivo*. However, the *in vivo* flow environment is rather complex (Goldsmith and Turitto, 1986). These complexities include the facts that 1) blood is not a dilute suspension, and the transport of a particular cell is influenced by the presence of other cells in the suspension (e.g., leukocyte and platelet transport to the vessel wall is influenced by the presence of red blood cells [Melder et al., 1995; Goldsmith and Turitto, 1986; Chien, 1982]); and 2) the blood vessels are of finite size, and the ratio of vessel diameter to particle diameter can affect the drag force on a particle near the wall (Schmid-Schoenbein et al., 1975; House and Lipowsky, 1988; Chapman and Cokelet, 1998). As a first step toward understanding the role of particle size in adhesion, we sought to investigate the role of particle diameter in adhesion under well-defined and controlled *in vitro* fluid flow conditions. To do this, we studied the adhesion of the 19.ek.Fc microspheres using a dilute suspension of microspheres in an *in vitro* parallel plate flow chamber. Although such an *in vitro* model does have its limitations (i.e., it clearly does not recreate all of the complexities of the *in vivo* environment discussed above), it is routinely used to gain insight into adhesion events that occur *in vivo* (Crutchfield et al., 2000; Lawrence et al., 1990; Lusinskas et al., 1994; Patel and McEver, 1997; Lawrence and Springer, 1991). In addition, our group (Goetz et al., 1997; Crutchfield et al., 2000) and Hammer's group (Brunk et al., 1996; Brunk and Hammer, 1997; Rodgers et al., 2000) have shown that key features of cellular

adhesion can be recreated using ligand-coated microspheres in a two-dimensional Poiseuille flow adhesion assay.

The initial step of particle adhesion to a substrate under flow is the attachment of the particle to the substrate from the fluid stream. To investigate attachment, 5-, 10-, 15-, and 20- μm 19.ek.Fc microspheres were perfused over P-selectin substrates at three different shear rates. At 75 s^{-1} , the percentage of 5-, 10-, 15-, and 20- μm -diameter microspheres that attached to the P-selectin surface were similar (Fig. 3 A). In contrast, at higher shear rates, there was a distinct dependence of the rate of attachment on the microsphere diameter. At the highest shear investigated, 600 s^{-1} (Fig. 3 C), only the 5- μm -diameter microspheres consistently exhibited appreciable attachment. Occasionally, a 10- μm microsphere would attach to the P-selectin surface at this shear rate. We never observed a 15- or 20- μm microsphere attach at this shear rate. ANOVA indicated that the rate of attachment was a function of the diameter of the microsphere at this shear rate. We next tested an intermediate shear rate. At 400 s^{-1} (Fig. 3 B), we did observe attachment of the 10- and 15- μm microspheres as well as the 5- μm microspheres. The 20- μm microspheres, however, did not attach at this shear rate. ANOVA indicated that the rate of attachment appeared to be a function of microsphere diameter at this shear rate ($p = 0.07$). Note that the microspheres were moving too fast at 400 and 600 s^{-1} to allow an accurate determination of the number of microspheres near the surface. Thus, we did not correct for the rate of delivery of the microspheres to the P-selectin substrate at these shear rates. Because the Stoke's settling velocity for a microsphere is proportional to the square of the diameter of the microsphere (Brenner, 1961), it is reasonable to assume that the rate of delivery of the 19.ek.Fc microspheres to the P-selectin substrate increases with increasing microsphere diameter (e.g., the rate of delivery of the 20- μm microspheres is greater than that of the 5- μm microspheres). This consideration suggests that the trends observed at 400 and 600 s^{-1} (Figs. 3, B and C) would be more pronounced if the rate of delivery were taken into account. Combined, the data in Fig. 3 clearly indicate that the microsphere diameter can affect the rate of attachment and this effect appears to be coupled to the level of fluid shear.

The shear stress required to set in motion a firmly adherent 19.ek.Fc microsphere decreases with increasing microsphere diameter

At the high concentrations of 19.ek.Fc and P-selectin used in this study, the majority of the 19.ek.Fc microspheres were firmly adherent at the lowest shear stress tested. As the shear stress was increased, a portion of the 19.ek.Fc microspheres would begin to roll (i.e., they would move in the direction of flow while remaining in contact with the substrate). To assess the role of particle diameter in firm

adhesion, we allowed the 19.ek.Fc microspheres to attach to the P-selectin-coated surface at 0.5 dynes/cm^2 . Subsequently, the shear stress was increased in a stepwise fashion, and the percentage of microspheres that continued to remain firmly adherent was determined. In general, the smaller microspheres were more likely to be firmly adherent compared to the larger microspheres (Fig. 4). For example, at 2 dynes/cm^2 , 100% of the 5- μm , $\sim 49\%$ of the 10- μm , $\sim 29\%$ of the 15- μm , and only $\sim 5\%$ of the 20- μm microspheres were firmly adherent. Multiple factor ANOVA indicated that the percent firmly adherent was a function of microsphere diameter and this effect was coupled to the level of fluid shear. Cozens-Roberts et al. (1990) defined the critical shear stress, S_c , as the shear stress required to remove 50% of a population of adherent particles. From the data presented in Fig. 4, we estimate S_c for the 20- μm microspheres to be $\sim 0.9\text{ dynes/cm}^2$, for the 15- μm microspheres to be $\sim 1.2\text{ dynes/cm}^2$, for the 10- μm microspheres to be $\sim 2\text{ dynes/cm}^2$, and for the 5- μm microspheres to be $\sim 5\text{ dynes/cm}^2$. These S_c values are plotted as a function of microsphere diameter in Fig. 5.

The rolling velocity increases with increasing microsphere diameter

We determined the rolling velocity of the 19.ek.Fc microspheres at various shear stresses (Fig. 6). In general, the larger microspheres rolled faster than the smaller microspheres. Note, for example, that, at 3 dynes/cm^2 , the rolling velocity of the 20- μm microspheres was $\sim 8.8\text{ }\mu\text{m/sec}$, of the 15- μm microspheres was $\sim 3.6\text{ }\mu\text{m/sec}$, of the 10- μm microspheres was $\sim 1.7\text{ }\mu\text{m/sec}$, and of the 5- μm microspheres was $\sim 0\text{ }\mu\text{m/sec}$. Multiple factor ANOVA indicated that the rolling velocity was a function of microsphere diameter and this effect was coupled to the level of fluid shear. We also found that the rolling velocity for all of the 19.ek.Fc microspheres increased with increasing shear stress and that the increase was dependent on the microsphere diameter. To illustrate this, for each set of 19.ek.Fc microspheres, we performed linear regression on the data presented in Fig. 6. The slope of the regression lines is the change of the rolling velocity with the shear stress. We then plotted these slopes as a function of microsphere diameter (Fig. 7). Linear regression of the data in Fig. 7 indicated that the slope was 0.21 and significantly different from zero. Thus, it appears that the rolling velocity increases with microsphere diameter, this effect is coupled to the level of fluid shear, and the change in the rolling velocity with shear stress is also a function of microsphere diameter.

DISCUSSION

Although theoretical arguments clearly suggest a role for cell diameter in adhesion, there have been very few exper-

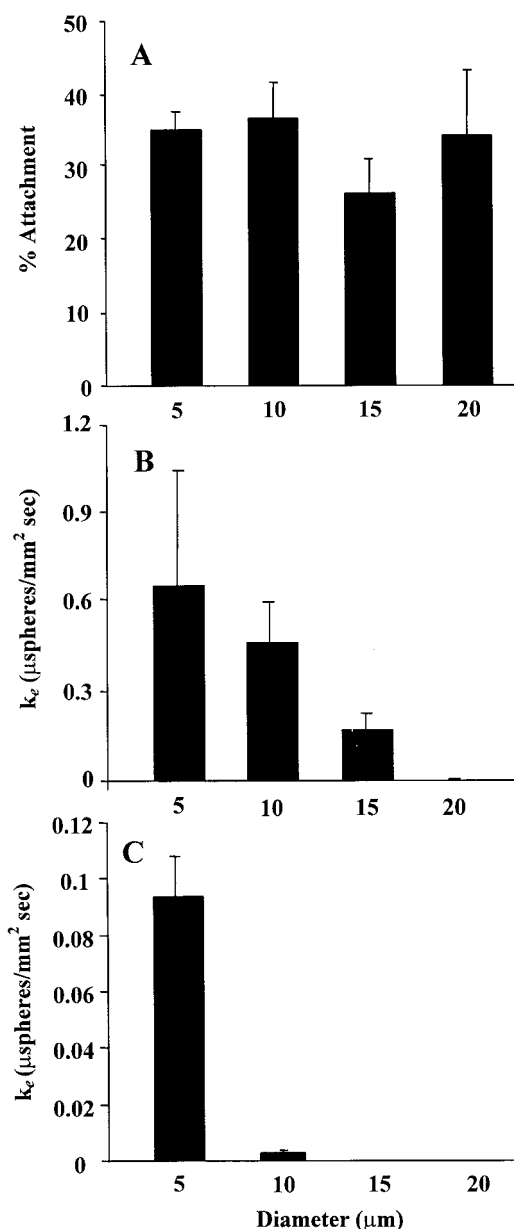


FIGURE 3 Comparison of the rates of attachment of 5-, 10-, 15-, and 20- μm 19.ek.Fc microspheres to P-selectin. (A) The effective rate of attachment of the 19.ek.Fc microspheres to the P-selectin substrate at 75 s^{-1} was determined. This value and an estimate of the number of 19.ek.Fc microspheres that passed through the field of view near the P-selectin-coated surface were used to determine the percentage of 19.ek.Fc microspheres that attached to the P-selectin substrate. At this shear rate, the percent attachment did not appear to be a function of the microsphere diameter ($p > 0.1$; $n \geq 4$). (B) The effective rate of attachment of the 19.ek.Fc microspheres to the P-selectin substrate at a shear rate of 400 s^{-1} was determined. At this shear, the rate of attachment appeared to be a function of the diameter of the 19.ek.Fc microspheres ($p = 0.07$; $n \geq 2$). (C) The effective rate of attachment of the 19.ek.Fc microspheres to the P-selectin substrate at a shear rate of 600 s^{-1} was determined. At this shear, the rate of attachment was a function of the diameter of the 19.ek.Fc microspheres. ($p < 0.05$; $n \geq 3$). Note that, in (B) and (C), the data were not corrected for the fact that the delivery of the 19.ek.Fc microspheres to the P-selectin surface is a function of the diameter of the microspheres. Because the Stoke's settling velocity is proportional to the square of the

experimental studies exploring this issue. In this study, we probed the role of cell diameter in adhesion by comparing the adhesion of 5-, 10-, 15-, and 20- μm -diameter 19.ek.Fc microspheres to P-selectin under in vitro flow conditions. We found that, for all adhesive states investigated (attachment, rolling, and firm adhesion), the adhesion was a function of the microsphere diameter.

We found that the attachment of 19.ek.Fc microspheres to P-selectin was a function of microsphere diameter and this effect was coupled to the fluid shear (Fig. 3). At high shear (600 s^{-1}), only the 5- μm -diameter 19.ek.Fc microspheres consistently exhibited appreciable levels of attachment (Fig. 3 C). At the lowest shear tested, there was little difference in the attachment (Fig. 3 A), and, at an intermediate shear, the rate of attachment appeared to decrease with increasing microsphere diameter (Fig. 3 B).

This trend could be explained by a variety of arguments including the idea that there are two different adhesion regimes operative over the range of shear rates tested (Chang and Hammer, 1999; Swift et al., 1998). At high shear, the adhesion may take place in a reaction-controlled regime, and, at low shear, the adhesion may be influenced by both transport and kinetics. A key parameter in this analysis is the slip velocity of the microspheres, which has been estimated as $\sim 0.47U$ (Chang and Hammer, 1999) where U is the translational velocity of the microsphere corrected for the wall effect (Goldman et al., 1967). Note that U is proportional to the particle diameter, and thus, the slip velocity increases with increasing particle diameter (Goldman et al., 1967). In the high shear, reaction-limited regime, a lower slip velocity favors adhesion (Swift et al., 1998; Chang and Hammer, 1999).

Another important parameter may be the contact area, which, from the analysis of Cozens-Roberts et al. (1990), increases with increasing particle diameter. Although what occurs in the transport-limited regime may be rather complex because several factors, in addition to contact area, may have an influence (e.g., particle and receptor diffusion [Goldsmith and Turitto, 1986; Chang and Hammer, 1999]), it could be argued that larger microsphere diameter favors adhesion because the larger microsphere will sample a larger area of the P-selectin substrate for the same length of substrate sampled.

Thus, a plausible explanation for the trend observed in Fig. 3 is that, at high shear, the adhesion takes place in a reaction-controlled regime. In this regime, smaller microsphere diameter is favorable for attachment because the smaller microspheres have a lower slip velocity compared to the larger microspheres. As the shear rate is decreased, reaction issues become less dominant and the transport

microsphere diameter, it is reasonable to assume that, if the delivery were taken into account, the trends observed in (B) and (C) would be more pronounced.

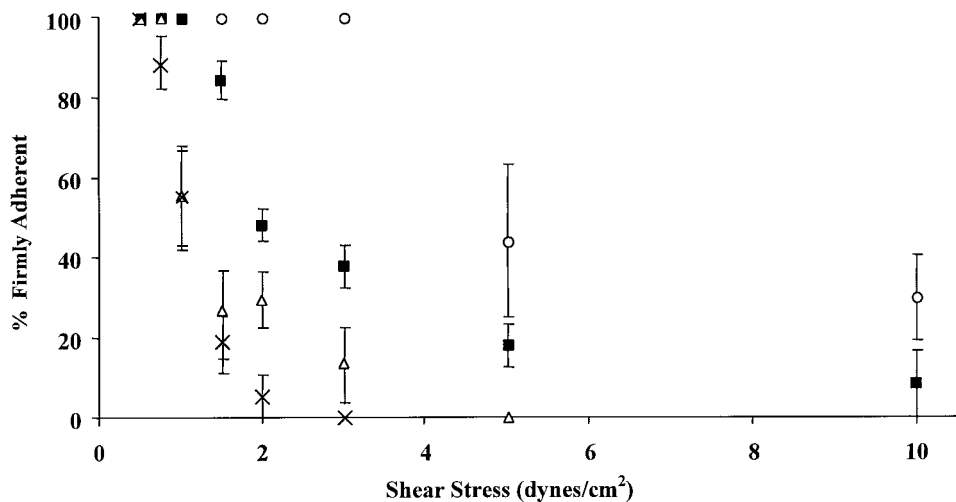


FIGURE 4 The shear stress required to set in motion a firmly adherent 19.ek.Fc microsphere decreases with increasing microsphere diameter. 5-, 10-, 15-, and 20- μm 19.ek.Fc microspheres were allowed to attach to the P-selectin substrate for 10 min at 0.5 dynes/cm². Subsequently, the shear stress was increased in a stepwise fashion. 19.ek.Fc microspheres that did not exhibit motion in the direction of flow were scored as firmly adherent. The percentage of firmly adherent 19.ek.Fc microspheres was plotted as a function of the shear stress. Multiple factor ANOVA indicated that percent firmly adherent was a function of microsphere diameter ($p < 0.01$) and this effect was coupled to the level of fluid shear ($p < 0.01$). (Legend: circles, 5- μm microspheres; boxes, 10- μm microspheres; triangles, 15- μm microspheres; crosses, 20- μm microspheres; $n \geq 5$ replicates are shown; Error bars, SEM).

begins to influence the attachment. As the attachment moves toward the transport-limited regime, the probability of a larger microsphere attaching becomes similar to the probability of smaller microsphere attaching, because, from a transport standpoint, the larger contact area of the larger microspheres relative to the smaller microspheres favors attachment.

In discussing the results of the firm adhesion data (Figs. 4 and 5), it is insightful to consider the analysis of Cozens-Roberts et al. (1990) with respect to the role of particle

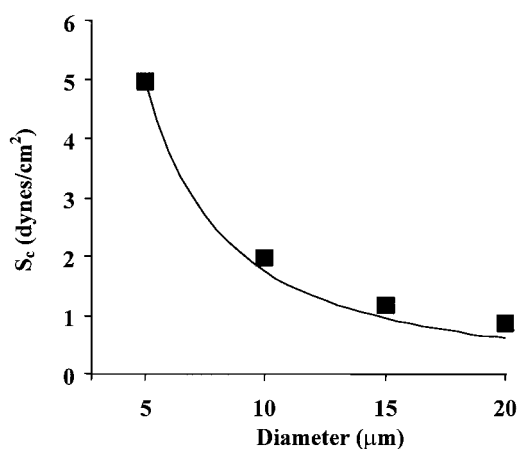
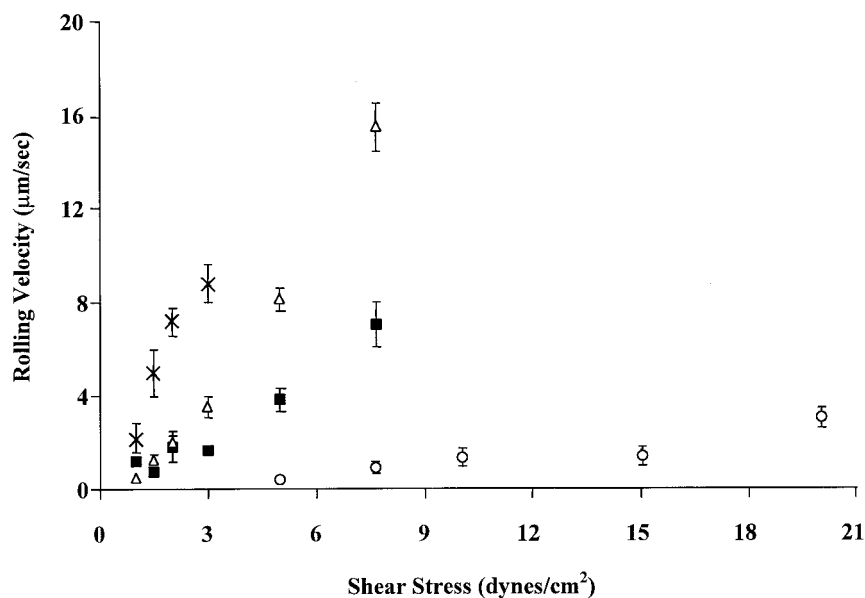


FIGURE 5 The critical shear, S_c , was estimated from the data shown in Fig. 4. These values were then plotted (black squares) as a function of microsphere diameter. The line depicts a theoretical curve developed as described in the Discussion section using the relationship of Cozens-Roberts et al. (1990), $S_c = K(\sin \Theta)^3$. Note that the experimental data closely follows the theoretical curve.

diameter in adhesion. As discussed in the introduction, increasing the particle diameter increases the disruptive force and torque exerted on an adherent particle by the fluid flow (Goldman et al., 1967) and the contact area between the particle and the substrate (Cozens-Roberts et al., 1990). The latter effect should be pro-adhesive, whereas the former is detrimental to adhesion. Cozens-Roberts et al. (1990) defined the critical shear stress, S_c , as the shear stress required to remove 50% of a population of adherent particles and developed a model to predict S_c as a function of a variety of factors including the particle diameter. Their analysis indicates that S_c is given by $K(\sin \Theta)^3$ where Θ is given by $\cos^{-1}[1 - (H - h_s)/\rho_B]$, h_s is the separation distance between the 19.ek.Fc microsphere and the P-selectin surface, ρ_B is the radius of the microsphere, and H is the maximum separation distance for 19.ek.Fc-P-selectin binding. For a fixed h_s and H , Θ , $\sin \Theta$, and, consequently, S_c decrease with increasing microsphere diameter. Thus, the net effect of an increase in microsphere diameter is a decrease in the level of shear stress needed to remove an adherent microsphere.

As would be predicted from this model (Cozens-Roberts et al., 1990), we observed that the shear stress required to set in motion a firmly adherent microsphere decreased with increasing microsphere diameter (Figs. 4 and 5). Using the analysis of Cozens-Roberts et al. (1990), it is possible to predict the change in S_c with particle diameter. We estimated K from the 5- μm microsphere data using $h_s = 10$ nm and $H = 40$ nm. We then plotted S_c versus microsphere diameter using this value of K and the equation $S_c = K(\sin \Theta)^3$. The resulting curve is given in Fig. 5 and is

FIGURE 6 The rolling velocity of the 19.ek.Fc microspheres increases with increasing microsphere diameter. The rolling velocity of the 19.ek.Fc microspheres that were not firmly adherent to the P-selectin substrate was determined. In general, the rolling velocity appears to increase with microsphere diameter. Multiple factor ANOVA indicated that the rolling velocity was a function of microsphere diameter ($p < 0.01$) and this effect was coupled to the level of fluid shear ($p < 0.01$). (Legend: circles, 5- μm microspheres; boxes, 10- μm microspheres; triangles, 15- μm microspheres; crosses, 20- μm microspheres. $n \geq 5$ separate experiments with ≥ 6 microspheres analyzed at each shear stress in a given experiment; Error bars, SEM).



shown to closely track the experimental data. The rolling velocity data also indicated that post-attachment adhesion decreased with increasing microsphere diameter (Fig. 6). In addition, the sensitivity of the rolling velocity to changes in fluid shear increased with increasing microsphere diameter (Fig. 7).

We have made a first step toward elucidating the role of particle size in adhesion. Several future investigations are quite evident from this initial study. First, as we noted in the Results section, the *in vitro* model we used in this study does not capture all of the complexities of the *in vivo* environment. *In vivo*, adhesion occurs in a tube of finite size, and the ratio of the tube diameter to the particle

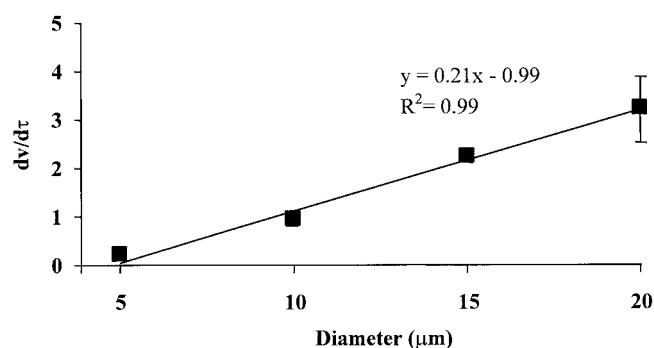


FIGURE 7 The change in the rolling velocity with fluid shear increases with microsphere diameter. Linear regression was performed on the data presented in Fig. 6. The slopes of these regression lines were plotted as a function of the microsphere diameter. Linear regression was performed on this data. The slope was found to be 0.21 ± 0.15 (slope \pm 95% confidence interval) indicating that the change in the rolling velocity with fluid shear significantly increases with increasing microsphere diameter. (Error bars indicate 95% confidence interval on slopes determined using regression on the data in Fig. 6.)

diameter can influence the drag force on a particle near the tube wall (Schmid-Schoenbein et al., 1975; House and Lipowsky, 1988; Chapman and Cokelet, 1998). It might be possible to investigate this issue with the *in vitro* model described here. For example, one could systematically alter the height of the flow chamber and the microsphere diameter to determine whether the ratio of the gap size to particle diameter affects the resulting adhesion. A second study of interest would be to apply pause time analysis (Alon et al., 1995; Smith et al., 1999) to the system described in the present study. Our data suggests that k_{off} increases with increasing particle diameter (Figs. 4, 5, and 6). One could test this hypothesis using pause time analysis. In addition, by varying the particle size in pause time experiments, one could gain insight into the tensile properties of ligand-receptor bonds. Such studies would be an excellent complement to existing data that has probed the tensile properties of ligand-receptor bonds by varying the shear stress. Finally, although we have given a plausible explanation of the attachment data (Fig. 3), other explanations could also be put forward. Notably, the scenario we outlined in the first part of the Discussion did not directly address the issue of bond strength. The interplay between bond strength, attachment, and particle size is likely quite complex given the fact that Evans's group (Evans, 1998; Evans and Ritchie, 1997) has demonstrated that increasing the rate of loading of a receptor-ligand bond may increase the strength of the bond. Obtaining a complete understanding of the role of particle size in attachment will clearly require several additional studies.

In summary, we have probed the role of particle diameter in receptor-ligand-mediated adhesion under fluid flow and found that, for all adhesive states tested, microsphere diameter affected the adhesion and that the effect of diameter

was coupled to the level of fluid shear. At relatively high shear, smaller microsphere diameter was favorable for attachment. At the lowest shear rate tested, however, there was little difference in the attachment between the different sized microspheres. The effect of an increase in the microsphere diameter on post-attachment adhesion was a decrease in shear stress required to set in motion an adherent microsphere and an increase in the rolling velocity of microspheres that were not firmly adherent.

The authors wish to thank Dr. Raymond T. Camphausen, Genetics Institute, Cambridge MA, for reagents and cell lines.

This work was supported by The National Science Foundation grant BES 9733542 (0096303) and The National Institutes of Health grant GM57640.

REFERENCES

- Alon, R., D. A. Hammer, and T. A. Springer. 1995. Lifetime of the P-selectin-carbohydrate bond and its response to tensile force in hydrodynamic flow. *Nature*. 374:539–542.
- Brenner, H. 1961. The slow motion of a sphere through a viscous fluid towards a plane surface. *Chem. Eng. Sci.* 16:242–251.
- Brunk, D. K., D. J. Goetz, and D. A. Hammer. 1996. Sialyl Lewis^x/E-selectin-mediated rolling in a cell-free system. *Biophys. J.* 71:2902–2908.
- Brunk, D. K., and D. A. Hammer. 1997. Quantifying rolling adhesion using a cell-free assay: E-selectin and its carbohydrate ligands. *Biophys. J.* 72:2820–2833.
- Chambers, A. F., I. C. MacDonald, E. E. Schmidt, S. Koop, V. L. Morris, R. Khokha, and A. C. Groom. 1995. Steps in tumor metastasis: new concepts from intravital videomicroscopy. *Cancer Metast. Rev.* 14:279–301.
- Chang, K. C., and D. A. Hammer. 1999. The forward rate of binding of surface-tethered reactants: effect of relative motion between two surfaces. *Biophys. J.* 76:1280–1292.
- Chapman, G. B., and G. R. Cokelet. 1998. Flow resistance and drag forces due to multiple adherent leukocytes in postcapillary vessels. *Biophys. J.* 74:3292–3301.
- Chien, S. 1982. Rheology in the microcirculation in normal and low flow states. *Adv. Shock Res.* 8:71–80.
- Cozens-Roberts, C., J. A. Quinn, and D. A. Lauffenburger. 1990. Receptor-mediated adhesion phenomena: model studies with the radial flow detachment assay. *Biophys. J.* 58:107–125.
- Crutchfield, K. L., V. R. S. Patil, C. J. Campbell, C. A. Parkos, J. R. Allport, and D. J. Goetz. 2000. CD11b/CD18-coated microspheres attach to E-selectin under flow. *J. Leuk. Biol.* 67:196–205.
- Dong, C., J. Cao, R. J. Struble, and H. H. Lipowsky. 1999. Mechanics of leukocyte deformation and adhesion to endothelium under shear flow. *Annal. Biomed. Eng.* 27:298–312.
- Evans, E. 1998. Energy landscapes of biomolecular adhesion and receptor anchoring at interfaces explored with dynamic force spectroscopy. *Faraday Discuss.* 111:1–16.
- Evans, E., and K. Ritchie. 1997. Dynamic strength of molecular adhesion bonds. *Biophys. J.* 72:1541–1555.
- Fredrickson, B. J., J. F. Dong, L. V. McIntire, and J. A. Lopez. 1998. Shear-dependent rolling on von Willebrand factor of mammalian cells expressing the platelet glycoprotein Ib-IX-V complex. *Blood*. 92:3684–3693.
- Frenette, P. S., R. C. Johnson, R. O. Hynes, and D. D. Wagner. 1995. Platelets roll on stimulated endothelium in vivo: an interaction mediated by endothelial P-selectin. *Proc. Natl. Acad. Sci. U.S.A.* 92:7450–7454.
- Giavazzi, R. 1996. Cytokine-mediated tumor-endothelial cell interaction in metastasis. *Curr. Topics Microbiol. Immunol.* 213:13–30.
- Goetz, D. J., B. K. Brandley, and D. A. Hammer. 1996a. An E-selectin-IgG chimera supports sialylated moiety dependent adhesion of colon carcinoma cells under fluid flow. *Ann. Biomed. Eng.* 24:87–98.
- Goetz, D. J., H. Ding, W. J. Atkinson, G. Vachino, R. T. Camphausen, D. A. Cumming, and F. W. Luscinskas. 1996b. A human colon carcinoma cell line exhibits adhesive interactions with P-selectin under fluid flow via a PSGL-1-Independent mechanism. *Am. J. Path.* 149:1661–1673.
- Goetz, D. J., D. M. Greif, R. T. Camphausen, S. Howes, K. M. Comess, K. R. Snapp, G. S. Kansas, and F. W. Luscinskas. 1997. Isolated P-selectin glycoprotein-1 dynamic adhesion to P- and E-selectin. *J. Cell Biol.* 137:509–519.
- Goldman, A. J., R. G. Cox, and H. Brenner. 1967. Slow viscous motion of a sphere parallel to a plane wall. II. Couette flow. *Chem. Eng. Sci.* 22:635–660.
- Goldsmith, H. L., and V. T. Turitto. 1986. Rheological aspects of thrombosis and haemostasis: basic principles and applications. *Thromb. Haemostasis.* 55:415–435.
- Gopalan, P. K., D. A. Jones, L. V. McIntire, and C. W. Smith. 1996. Cell adhesion under hydrodynamic flow conditions. In *Current Protocols in Immunology*. J. E. Coligan, A. M. Kruisbeek, D. H. Margulies, E. M. Shevach, and W. Strober, editors. J. Wiley, New York. 7.29.1–7.29.23.
- Hammer, D. A., and S. M. Apte. 1992. Simulation of cell rolling and adhesion on surfaces in shear flow: general results and analysis of selectin-mediated neutrophil adhesion. *Biophys. J.* 62:35–57.
- Hammer, D. A., and D. A. Lauffenburger. 1987. A dynamical model for receptor-mediated cell adhesion to surfaces. *Biophys. J.* 52:475–487.
- House, S. D., and H. H. Lipowsky. 1988. In vivo determination of the force of leukocyte-endothelium adhesion in the mesenteric microvasculature of the cat. *Circ. Res.* 63:658–668.
- Lawrence, M. B., D. F. Bainton, and T. A. Springer. 1994. Neutrophil tethering to and rolling on E-selectin are separable by requirement for L-selectin. *Immunity*. 1:137–145.
- Lawrence, M. B., C. W. Smith, S. G. Eskin, and L. V. McIntire. 1990. Effect of venous shear stress on CD18-mediated neutrophil adhesion to cultured endothelium. *Blood*. 75:227–237.
- Lawrence, M. B., and T. A. Springer. 1991. Leukocytes roll on a selectin at physiologic flow rates: distinction from and prerequisite for adhesion through integrins. *Cell*. 65:859–873.
- Luscinskas, F. W., G. S. Kansas, H. Ding, P. Pizcueta, B. E. Schleiffenbaum, T. F. Tedder, and M. A. Gimbrone, Jr. 1994. Monocyte rolling, arrest, and spreading on IL-4-activated vascular endothelium under flow is mediated via sequential action of L-selectin, β 1-integrins, and β 2-integrins. *J. Cell Biol.* 125:1417–1427.
- McCarty, O. J., S. A. Mousa, P. F. Bray, and K. Konstantopoulos. 2000. Immobilized platelets support human colon carcinoma cell tethering, rolling, and firm adhesion under dynamic flow conditions. *Blood*. 96:1789–1797.
- Melder, R. J., L. L. Munn, S. Yamada, C. Ohkubo, and R. K. Jain. 1995. Selectin- and integrin-mediated T-lymphocyte rolling and arrest on TNF- α -activated endothelium: Augmentation by erythrocytes. *Biophys. J.* 69:2131–2138.
- Munn, L. L., R. J. Melder, and R. K. Jain. 1995. Analysis of cell flux in the parallel plate flow chamber: implications for cell capture studies. *Biophys. J.* 67:889–895.
- Patel, K. D., and R. P. McEver. 1997. Comparison of tethering and rolling of eosinophils and neutrophils through selectins and P-selectin glycoprotein ligand-1. *J. Immunol.* 159:4555–4565.
- Rodgers, S. D., R. T. Camphausen, and D. A. Hammer. 2000. Sialyl Lewis^x-mediated, PSGL-1-independent rolling adhesion on P-selectin. *Biophys. J.* 79:694–706.
- Ross, R. 1999. Atherosclerosis—an inflammatory disease. *N. Engl. J. Med.* 340:115–126.
- Sako, D., X. J. Chang, K. M. Barone, G. Vachino, H. M. White, G. Shaw, G. M. Veldman, K. M. Bean, T. J. Ahern, B. Furie, D. A. Cumming, and

- G. R. Larsen. 1993. Expression cloning of a functional glycoprotein ligand for P-selectin. *Cell*. 75:1179–1186.
- Sako, D., K. M. Comess, K. M. Barone, R. T. Camphausen, D. A. Cumming, and G. D. Shaw. 1995. A sulfated peptide segment at the amino terminus of PSGL-1 is critical for P-selectin binding. *Cell*. 83:323–331.
- Scherbarth, S., and F. W. Orr. 1997. Intravital videomicroscopic evidence for regulation of metastasis by the hepatic microvasculature: effects of interleukin-1 α on metastasis and the location of B16–F1 melanoma cell arrest. *Can. Res.* 57:4105–4110.
- Schmid-Schoenbein, G. W., Y. C. Fung, and B. W. Zweifach. 1975. Vascular endothelium-leukocyte interaction; sticking shear force in venules. *Circ. Res.* 36:173–184.
- Smith, M. J., E. L. Berg, and M. B. Lawrence. 1999. A direct comparison of selectin-mediated transient, adhesive events using high temporal resolution. *Biophys. J.* 77:3371–83.
- Springer, T. A. 1994. Traffic signals for lymphocyte recirculation and leukocyte emigration: the multistep paradigm. *Cell*. 76:301–314.
- Swift, D. G., R. G. Posner, and D. A. Hammer. 1998. Kinetics of adhesion of IgE-sensitized rat basophilic leukemia cells to surface-immobilized antigen in Couette flow. *Biophys. J.* 75:2597–2611.
- von Andrian, U. H., S. R. Hasslen, R. D. Nelson, S. L. Erlandsen, and E. C. Butcher. 1995. A central role for microvillous receptor presentation in leukocyte adhesion under flow. *Cell*. 82:989–999.
- Wattenbarger, M. R., D. J. Graves, and D. A. Lauffenburger. 1990. Specific adhesion of glycophorin liposomes to a lectin surface in shear flow. *Biophys. J.* 57:765–777.